Results in Optics 5 (2021) 100115

Contents lists available at ScienceDirect

Results in Optics

journal homepage: www.sciencedirect.com/journal/results-in-optics

Q-switched mode locking noise-like pulse generation from a thulium-doped all-fiber laser based on nonlinear polarization rotation

R. López-Estopier [a,b], A. Camarillo-Avilés [a], M. Bello-Jiménez [a,*], O. Pottiez [c], M. Durán-Sánchez [b,d], B. Ibarra-Escamilla [d], E. Rivera-Pérez [e], M.V. Andrés [f]

[a] Instituto de Investigación en Comunicación Óptica, Universidad Autónoma de San Luis Potosí, Av. Karakorum No. 1470 Lomas 4ª Secc., 78210 San Luis Potosí, Mexico
[b] Consejo Nacional de Ciencia y Tecnología (CONACYT), Av. Insurgentes Sur No. 1582, Col. Crédito Constructor, Del. Benito Juárez, 039040 Ciudad de México, Mexico
[c] Centro de Investigaciones en Óptica (CIO), Loma del Bosque No. 115, Col. Lomas del Campestre, 37150 León, Guanajuato, Mexico
[d] Instituto Nacional de Astrofísica, Óptica y Electrónica (INAOE), Luis Enrique Erro No. 1, Departamentode Óptica, 72000 Puebla, Mexico
[e] Departamento de Física, Universidad de Guanajuato, Loma del Bosque 103, 37150 León, Guanajuato, Mexico
[f] Universidad de Valencia, Departamento de Física Aplicada y Electromagnetismo, ICMUV, c/Dr. Moliner 50, Burjassot, 46100 Valencia, Spain

ARTICLE INFO

Keywords:
Q-switched mode locking
Thulium-doped fiber lasers
Nonlinear polarization rotation

ABSTRACT

Q-switched mode locking (QML) noise-like pulse (NLP) emission from an all-fiber thulium-doped laser based on the nonlinear polarization rotation effect is reported. The QML emission is obtained in a cavity with net anomalous dispersion in a pump power interval in between the CW laser threshold and the threshold of the NLP regime. Highest-energy QML pulses were observed with a repetition rate of 812 kHz with a pump power of 520 mW at the optical wavelength of 1881.09 nm. A maximum overall energy of 460 nJ at an average output power of 6.4 mW was reached, which corresponds to a burst of mode-locked noise-like sub-pulses with 8.7 ns of pulse duration within a QML envelope of 11 μs. These results demonstrate unconventional pulse operation regime of NLPs and provide insights into the dynamics of mode-locked fiber lasers.

1. Introduction

Pulsed fiber lasers operating in the 2-μm spectral region have become essential optical light sources in diverse fields of science and industry, especially where parameters such as power, safety, accuracy, and precision are issues of paramount importance (Bremer et al., 2013; Camarillo-Avilés et al., 2021; Fried and Murray, 2005; Gaida et al., 2018; Hardy et al., 2014; Huang et al., 2016; Kalaycıoğlu et al., 2017; Kronenberg and Traxer, 2019; Lekarev et al., 2020; Liang et al., 2018; Liao et al., 2018; Mingareev et al., 2016; Olson et al., 2018; Ren et al., 2019; Swiderski et al., 2021; Traxer and Keller, 2019; Ventimiglia et al., 2020; Zeng et al., 2019; Traxer et al., 2019; Voisiat et al., 2015). Their most common applications include research areas such as laser spectroscopy (Liao et al., 2018; Olson et al., 2018), medical treatment (Fried and Murray, 2005; Hardy et al., 2014; Huang et al., 2016; Kronenberg and Traxer, 2019; Lekarev et al., 2020; Traxer and Keller, 2019; Ventimiglia et al., 2020; Traxer et al., 2019), material processing (Mingareev et al., 2016; Kalaycıoğlu et al., 2017; Voisiat et al., 2015) and optical sensing (Bremer et al., 2013), among others (Camarillo-Avilés et al., 2021; Zeng et al., 2019; Swiderski et al., 2021; Gaida et al., 2018; Liang et al., 2018; Ren et al., 2019). In those approaches, there are essentially two well-known techniques for optical pulse generation. One of them is the mode locking (ML) technique, which is the preferred method to generate short or ultrashort optical pulses in a range from a few tens of picoseconds to several hundreds of femtoseconds. In addition, ML can be implemented to perform high pulse repetition frequencies and superior stability (Ahmad et al., 2018; Wang et al., 2018). The other technique, which is referred to as Q switching (QS), is the preferred method to generate high-energy and relatively long optical pulses. It relies on modulating the Q factor of the cavity to produce an abrupt photon emission. This method mainly generates high energy Gaussian pulses with nanosecond pulse durations and repetition rates of the order of kilohertz (kHz) (Ibarra-Escamilla et al., 2018; Wang et al., 2019; Ahmad et al., 2018). Nevertheless, and despite the advantages of these techniques, an alternative hybrid method named Q-switched mode locking (QML) could be implemented to combine the best characteristics of ML and QS emissions, generating a burst of ML sub-pulses within a large QS envelope. In this way, this method provides additional energy to the ML sub-pulses and significantly increments the peak power. Therefore, the QML technique is a very attractive solution to enhance the output

* Corresponding author.
E-mail address: miguel.bello@uaslp.mx (M. Bello-Jiménez).

https://doi.org/10.1016/j.rio.2021.100115
Received 12 May 2021; Received in revised form 21 June 2021; Accepted 29 June 2021
Available online 7 July 2021

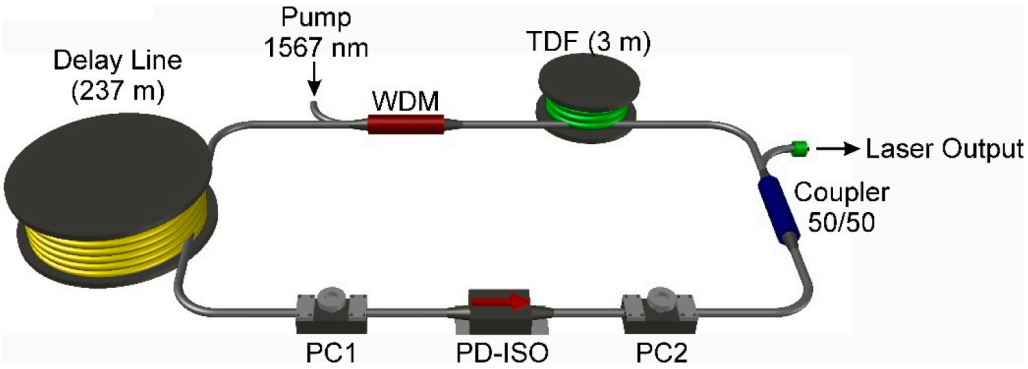

Fig. 1. Schematic of the QML thulium-doped all-fiber laser.

emission without requiring additional high-power amplification (Ma et al., 2018; Shtyrkova et al., 2019).

In the last decade, a different type of pulse emission, commonly referred to as noise-like pulse (NLP), have attracted the attention of researchers due to their unique properties in the spectral and temporal domains. The most distinguished feature of NLPs is the emission of nanosecond-scale optical pulses, whose composition consists of an inner structure of ultrashort optical pulses with random peak amplitude and duration, together with a broad and smooth average optical spectrum. At present, several schemes for NLP emission have been reported to investigate their properties, such as their internal structure, different pulse shaping or complex dynamics in the spectral and temporal regimes, simply by controlling some of the cavity parameters like fiber dispersion, gain, cavity loss, polarization, and nonlinearity (Liu et al., 2016; Michalska and Swiderski, 2019; Zhao et al., 2018; Ahmad et al., 2020). Therefore, novel features and unprecedented behaviors of NLPs are still expected to emerge and play an important role in the photonics field. Following this research line, NLP emission does not seem to require a fine adjustment of the cavity parameters, and they can be found over a wide variety of fiber laser architectures, operation wavelengths and dispersion regimes (Chen et al., 2016; Wang et al., 2021; Bracamontes-Rodríguez et al., 2017). For a cavity operating through the nonlinear polarization rotation technique, polarization defines the nonlinear transmission of the passive mode locker. Therefore, it is common to access to a NLP regime by properly adjusting the pressure and orientation of the polarization controllers (Camarillo-Avilés et al., 2021; Lin et al., 2016; Durán-Sánchez et al., 2021). This manuscript focuses on reporting for the first time a Q-switched mode locked noise-like pulse emission from a thulium-doped all-fiber laser with passive saturable absorption action. The evolution of QML noise-like pulses is experimentally investigated and the results demonstrate the feasibility of a different type of NLP operation in a mode-locked fiber laser.

In this work a noise-like pulse source operating around the 2-μm spectral region is reported and its capability to generate QML noise-like pulses in a thulium-doped laser is demonstrated based on the nonlinear polarization effect. The experimental results demonstrate the potential of the proposed scheme to generate a burst of mode-locked noise-like sub-pulses of 8.71 ns pulse duration within a QML envelope of 11 μs. These results, to the best of our knowledge, could be considered as the first demonstration of QML noise-like generation around the 2-μm spectral band and unveil a new facet of the complexity of NLP operation in mode-locked fiber lasers.

2. Experimental setup

A schematic view of the experimental setup is shown in Fig. 1. The gain medium is provided by a 3-m long of thulium doped fiber (TDF) (CorActive SCF-TM-8/125) with a core diameter of 8 ± 1 μm and numerical aperture of 0.17 ± 0.01. The TDF was pumped by a 1567 nm fiber laser source through a 1550/2000 nm wavelength division multiplexer (WDM). The maximum pump power delivered into the TDF was 1.73 W. The WDM is also connected to a delay line of 237 m in length (Thorlabs SM-2000 fiber). This delay line is required in our setup to facilitate the mode locking operation. Then, a polarization-dependent isolator (PD-ISO) is connected between two in-line polarization controllers (PC_1 and PC_2), allowing to perform the saturable absorption action through the nonlinear polarization rotation (NPR) effect. The ring cavity is closed by splicing one transmission port of a 50/50 fiber coupler to one end of the TDF. The remaining transmission port is used to obtain the laser output through the fiber coupler. The total length of the cavity was measured as ~255.61 m, which is composed of 240.33 m SM-2000 fiber, 3 m of TDF and 12.28 m of SMF-28 fiber. The cavity round-trip time is expected to be ~1.23 μs, together with a fundamental repetition rate of ~812.78 kHz. A rough estimation of the cavity dispersion was carried out by considering the dispersion values reported in (Li et al., 2014), where anomalous dispersion values of −84 ps^2/km, −73 ps^2/km and −80 ps^2/km are reported for the SM-2000, thulium-doped and SMF-28 fibers, respectively. Thus, the average cavity dispersion is estimated as −83.67 ps^2/km, obtaining a net cavity dispersion of −21.39 ps^2.

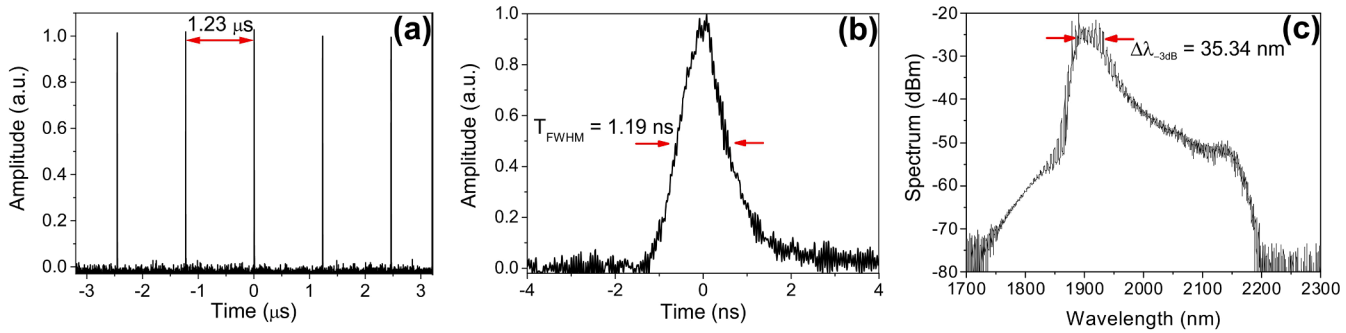

Fig. 2. (a) Optical pulse train with period of 1.23 μs. (b) Output pulse with pulse duration of 1.19 ns. (c) Output spectrum with 3-dB optical bandwidth of 35.34 nm.

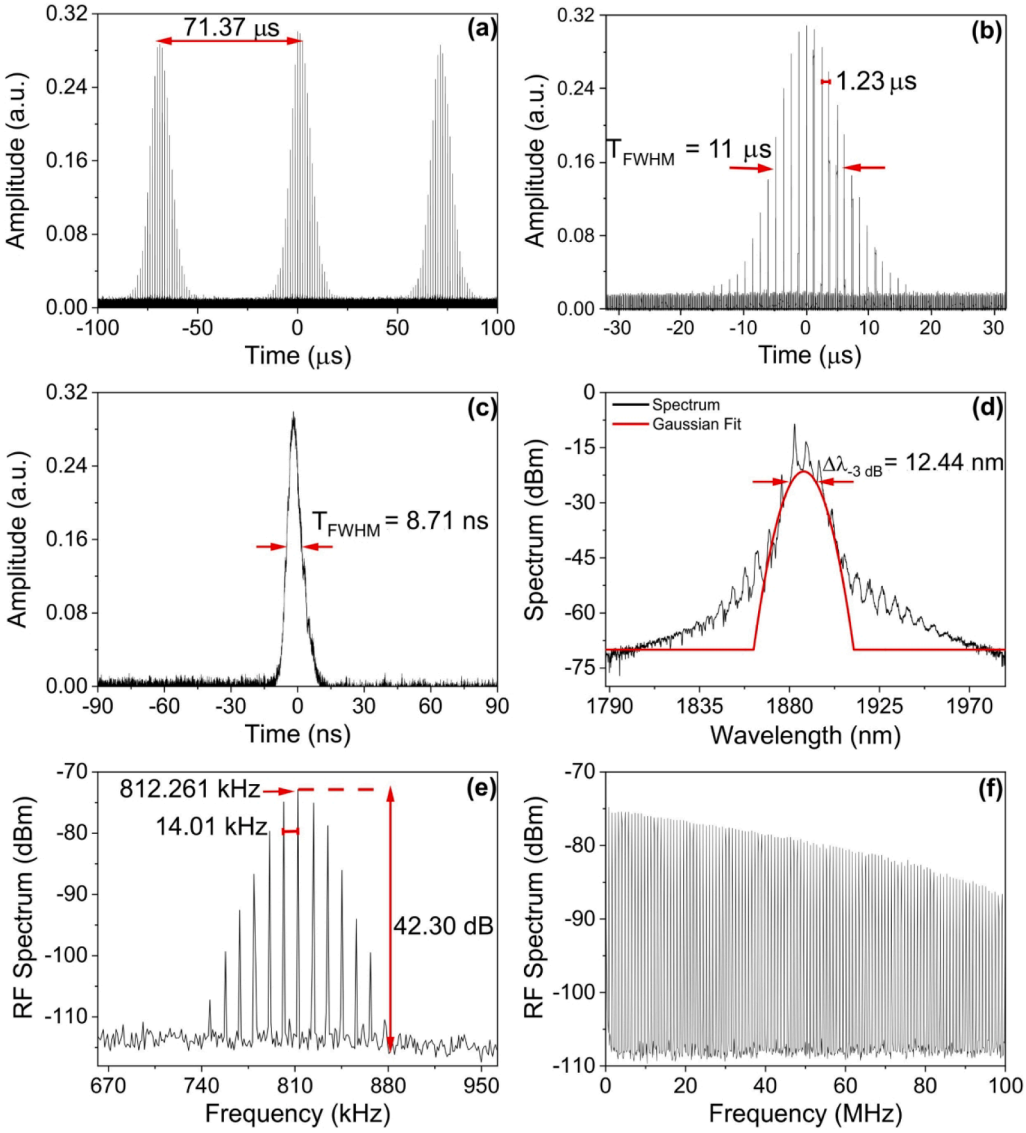

Fig. 3. (a) QML pulse train output with period of 71.37 µs. (b) Close-up view of the QML pulse. (c) Measurement of the ML central sub-pulse. (d) Measured optical spectrum in QML operation. (e) RF spectra of the output pulses. (f) RF spectrum with 100 MHz frequency span and 30 Hz RBW.

Pulsed light emission was monitored by using a 10 GHz photodetector (Newport 818-BB-51F, wavelength range 830–2150 nm and 28 ps rise time) and a 20-GHz real-time oscilloscope (Tektronix DPO72004C). The spectral properties were analyzed by an optical spectrum analyzer (OSA, Yokogawa AQ6375, scanning range from 1200 to 2400 nm and 50 pm of maximum resolution) along with a 3.2-GHz electrical spectrum analyzer (ESA, Siglent SSA3032X, 10 Hz of resolution bandwidth).

3. Experimental results and discussion

Pulse emission is achieved under different laser operating regimes, such as conventional soliton and noise-like pulses. Here, we focused on the mode-locked NLP regime, which is characterized by the emission of nanosecond-scale pulse widths and a broad optical spectrum. By carefully adjusting the PCs and gradually incrementing the pump power, NLP operation is achieved with a minimum pump power of 520 mW. Fig. 2(a) illustrates the generated train of NLPs exhibiting a pulse interval of 1.23 µs. This value is equivalent to the fundamental round-trip time of the 255.61-m long cavity. A close-up view of a single-shot NLP is depicted in Fig. 2(b), where a full width at half maximum (FWHM) of 1.19 ns is calculated. A measurement of the corresponding optical spectrum is shown in Fig. 2(c), where a broad and smooth optical spectrum with 3-dB optical bandwidth of 35.34 nm and peak amplitude located at 1902 nm is obtained. The spectrum also reveals fine oscillation peaks around the 1900 nm region, which are essentially attributed to the molecular resonances of CO_2 and water (Olson et al., 2018; Rothman et al., 2013). From these results, although it was not possible to obtain the specific autocorrelation trace for the output pulses, it can be observed the two main characteristics of NLP emission: a long pulse emission together with a and broad optical spectrum (Durán-Sánchez et al., 2020; Guo et al., 2018; Wang et al., 2017). Therefore, it is deduced from the temporal and spectral measurements that the laser operates in the NLP emission regime. Stable NLP operation is observed in a range of pump power between 520 and 1281 mW, over which the pulse duration (FWHM) increases from 1.19 to 2.19 ns and the −3-dB optical bandwidth from 35.34 to 92.86 nm, respectively. For these results, the measurements were carried out maintaining fixed the PCs and only incrementing the pump power throughout the experimental process.

One interesting feature of the present scheme arises by reducing the pump power below the lasing threshold of continuous-wave (CW) mode-locked NLPs and readjusting the PCs. Under this procedure, the conventional NLP emission gradually disappears and evolve into a Q-

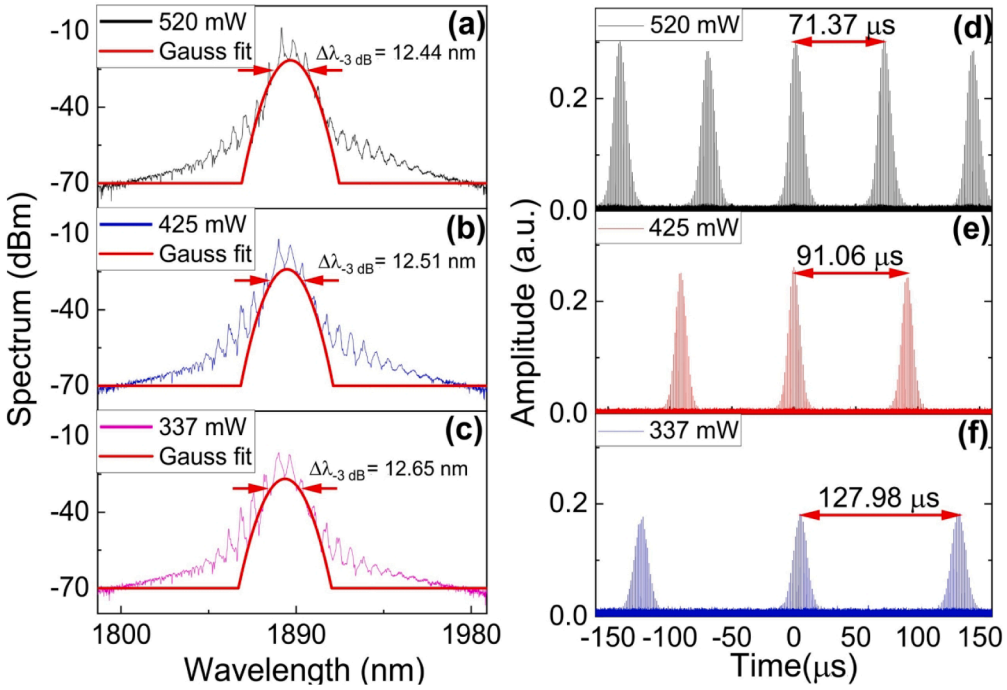

Fig. 4. Optical spectrum (a) - (c) and QML pulse train (d) - (f) as a function of pump power in a range between 337 and 520 mW.

switched mode-locked (QML) pulse operation. The range of pump power that sustains a stable QML noise-like pulse operation was found to be between 337 and 520 mW. The optimal emission was achieved by fixing the pump power at 520 mW and carefully modifying the cavity loss via the PCs. In this manner, an alteration of the PCs orientation induces a change of the intracavity polarization state that leads to an elaborate nonlinear response based on the NPR effect. Q-switched mode-locked NLP emission could be attributed to the non-stationary behavior of NLPs, that leads to a quasi-periodic instability related to a particular "Q-switched-like" operation that is described in several publications (Pottiez et al., 2017; Ibarra Villalón et al., 2018; Smirnov et al., 2017; Wang et al., 2018, 2016). Therefore, we believe that this instability around the CW-NLP lasing threshold induce an additional intracavity modulation that is related to the Q switching phenomenon, giving rise to the

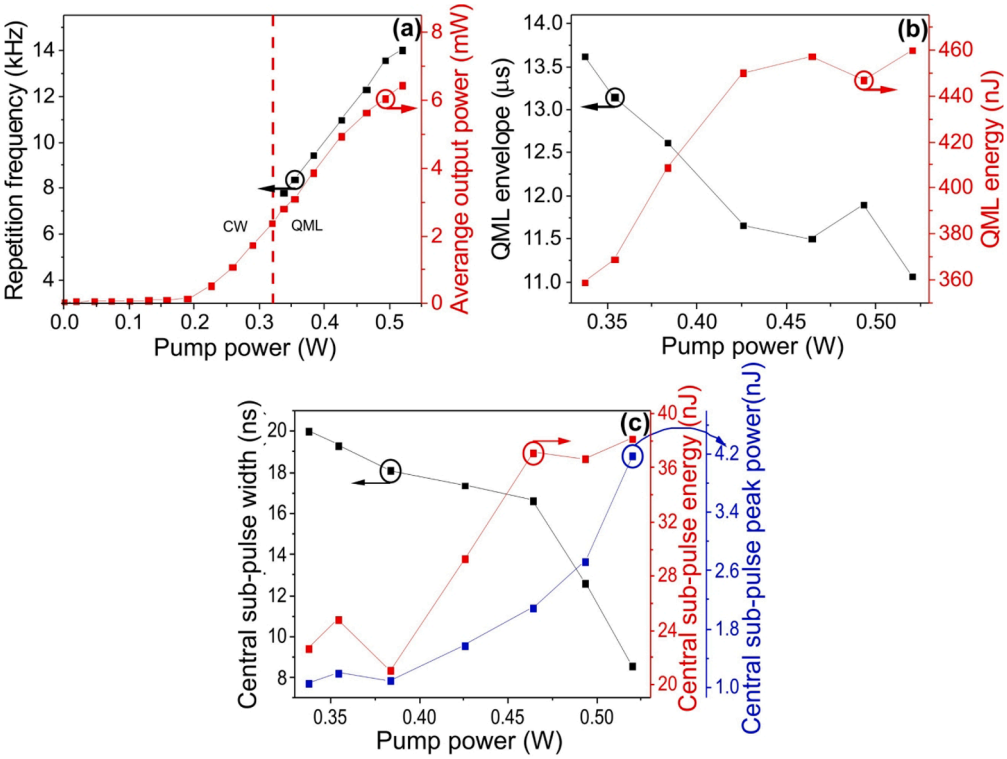

Fig. 5. Characteristics of QML noise-like pulses as a function of pump power. (a) Repetition frequency and average output power. (b) QML pulse envelope and energy. (c) Central ML sub-pulse width, energy, and peak power.

combined effect of Q switching and mode locking NLP emissions. Fig. 3 (a) illustrates the train of QML noise-like pulses at the laser output, where a Q-switching repetition period of 71.37 μs is observed. A more detailed view for a single QML noise-like pulse is presented in Fig. 3(b), in which a FWHM for the QS envelope of 11 μs is estimated. The inner structure of ML sub-pulses possesses a time separation of 1.23 μs, equivalent to the fundamental cavity round-trip time. A close-up view of a single mode-locked NLP sub-pulse is shown in Fig. 3(c), exhibiting a nanosecond pulse width (FWHM) of 8.71 ns. Fig. 3(d) illustrates the corresponding optical spectrum of the QML emission. A −3 dB optical bandwidth of 12.44 nm with a peak amplitude located at 1881.09 nm was measured. If we compare these results with the NLP emission reported in Fig. 2, the QML emission preserves a broad optical bandwidth, together with nanosecond scale ML optical pulses, indicating that the laser operates in a QML noise-like pulse regime. We also observed that NLP pulse duration is larger and spectrum narrower in the QML regime, compared to the Fig. 2. However, peak oscillations are observed in the spectrum, which are not to be mistaken for Kelly sidebands, considering their uniform spacing. In order to verify the origin of this phenomenon, the spectrum of conventional NLP emission was measured under similar conditions. It was found that oscillations also exist in the spectrum and concentrate around the 1900 nm region, as shown in Fig. 2(c), These amplitude oscillations may be attributed to some interferometric effect produced by reflections between the OSA detector and the fiber connector when the measurement was carried out. The RF spectrum, measured with 280 kHz span and 10 Hz resolution bandwidth, is depicted in Fig. 3(e). It displays a center peak at the fundamental frequency of 812.26 kHz with a signal-to-noise ratio (SNR) of 49.10 dB. This frequency is equivalent to the inverse period of 1.23 μs for the ML sub-pulses. In addition, multiple bands on both sides of the center peak with uniform interval of ± 14.01 kHz agree with the repetition period of 71.37 μs, which corresponds with the QML emission. An extended view of the harmonic frequency signals over a frequency span of 100 MHz and 30 Hz resolution bandwidth (RBW) is shown in Fig. 3(f). A minimum SNR of ~25 dB is observed in the wide RF spectrum, revealing a good stability of the fiber laser.

The evolution of the optical spectrum and the QML noise-like pulse train under different pump power levels are shown in Fig. 4. This set of measurements were performed maintaining fixed the PCs and only varying the pump power throughout the experimental process. By increasing the pump power from 337 to 520 mW, the −3 dB bandwidth of the optical spectrum decreases slightly from 12.65 nm to 12.44 nm, as shown in the Fig. 3(a) to (c), where a Gaussian fit was used as a reference (red trace). Similarly, the corresponding oscilloscope traces shown in Fig. 3(d) to (f), illustrate a reduction of the repetition period when applying the same pump power variation. For the pump power values of 337, 425 and 520 mW, the time interval of QML envelope takes the values of 127.98, 91.06 and 71.37 μs, respectively. This latter behavior is characteristic of conventional passively Q switched pulse operation.

The variations of repetition frequency and of average output power of QML noise-like pulse emission with pump power are presented in Fig. 5(a). For the pump power interval between 337 mW and 520 mW, the repetition frequency increments from 7.813 kHz to 14.01 kHz, respectively. The CW laser threshold is observed at 225 mW, above this level the laser operates in a continuous-wave regime and switches to a QML noise-like pulse emission at 337 mW of pump power, reaching an average output power of 2.80 mW. A maximum average output power of 6.44 mW was obtained at the maximum pump power of 520 mW. The evolutions of QML pulse envelope duration and pulse energy are shown in Fig. 5(b). The QML envelope undergoes a decreasing behavior, experiencing a pulse width (FWHM) reduction from 13.62 to 11.06 μs. In contrast, the corresponding pulse energy increments from 359.27 to 459.81 nJ over the same pump power interval. Fig. 5(c) illustrates the behavior of the central ML sub-pulse. By setting the pump power at 337 mW the pulse width and energy were measured as 20.05 ns and 22.64 nJ, respectively. However, by increasing the pump power to 520 mW, the energy of the sub-pulse increased to 38.15 nJ and its temporal width decreased to 8.57 ns. These evolutions contrast with the typical behavior of continuous-wave NLPs, whose duration is usually found to increase linearly with pump power, whereas their amplitude remains constant, as reported in numerous experimental works (Liu et al., 2015, 2017; Wang et al., 2021). Through this result, it can be concluded that the most energetic ML central sub-pulse is obtained with the smallest temporal width. The overall energy was estimated using the numerical integral of the oscilloscope traces, from which a peak power ranging from 1.06 to 4.17 W is measured for the central ML noise-like sub-pulse. If we compare the energy of the central ML NLP sub-pulse (38.15 nJ) with the conventional CW-NLP reported in Fig. 2(b), where a NLP energy of 4.82 nJ was generated at the same pump power of 520 mW, there is an improvement by almost a factor of 8 for the central QML noise-like pulse. This set of results demonstrate a different pulse operation regime for NLPs, which could be of great potential for practical applications in fiber lasers systems.

4. Conclusion

In this work the implementation of a thulium-doped all-fiber that allows the generation of QML noise-like pulses is demonstrated around the 2-μm spectral region. QML pulses were generated by the implementation of the nonlinear polarization rotation effect in a ring cavity. By carefully adjusting the PCs and regulating the pump power, QML noise-like operation is achieved with a minimum pump power of 337 mW. The best pulsed emission was obtained with a pump power of 520 mW, with a repetition rate of 812.26 kHz and optical wavelength of 1881.09 nm. In that case, the maximum energy and average output power were measured at 459.81 nJ and 6.44 mW, respectively, corresponding to a burst of ML sub-pulses of 8.71 ns pulse width within a 11 μs QML envelope. Although some features of the QML NLP emission evidenced in this work, such as the increase of the envelope repetition frequency with pump power, are shared with conventional passively Q-switched regimes, and thus have been studied and understood previously, other features, such as the decreasing duration and increasing intensity of the NLPs, are proper to this particular regime, and their detailed understanding will require further investigation. Hence, we believe these results contribute to a further developing the research of NLPs and its dynamics in mode-locked fiber lasers.

Declaration of Competing Interest

The authors declare that they have no known competing financial interests or personal relationships that could have appeared to influence the work reported in this paper.

Acknowledgement

This work was supported by CONACyT “Ciencia de Frontera 2019” under Grant 217560 and FAI-UASLP project C20-FAI-10-28.28.

References

Ahmad, H., Samion, M.Z., Yusoff, N., 2018. Soliton mode-locked thulium-doped fiber laser with cobalt oxide saturable absorber. Opt. Fiber Technol. 45, 122–127. https://doi.org/10.1016/j.yofte.2018.07.012.

Ahmad, H., Samion, M.Z., Sharbirin, A.S., Ismail, M.F., Zulkifli, M.Z., Thambiratnam, K., 2018. 70 nm, broadly tunable passively Q-switched thulium-doped fiber laser with few-layer Mo0. 8W0. 2S2 saturable absorber. Opt. Fiber Technol. 46, 230–237. https://doi.org/10.1016/j.yofte.2018.10.018.

Ahmad, H., Ahmed, M.H.M., Samion, M.Z., 2020. Generation of mode-locked noise-like pulses in double-clad Tm-doped fibre laser with nonlinear optical loop mirror. J. Mod. Opt. 67 (2), 146–152. https://doi.org/10.1080/09500340.2019.1699969.

Bracamontes-Rodríguez, Y.E., Pottiez, O., García-Sánchez, E., Lauterio-Cruz, J.P., Ibarra-Villalón, H.E., Hernandez-Garcia, J.C., Bello-Jimenez, M., Beltrán-Pérez, G., Ibarra-Escamilla, B., Kuzin, E.A., 2017. Dual noise-like pulse and soliton operation of a fiber ring cavity. J. Opt. 19 (3), 035502. https://doi.org/10.1088/2040-8986/aa5a41.

Bremer, K., Pal, A., Yao, S., Lewis, E., Sen, R., Sun, T., Grattan, K.T.V., 2013. Sensitive detection of CO 2 implementing tunable thulium-doped all-fiber laser. Appl. Opt. 52 (17), 3957–3963. https://doi.org/10.1364/AO.52.003957.

Camarillo-Avilés, A., López-Estopier, R., Pottiez, O., Durán-Sánchez, M., Ibarra-Escamilla, B., Bello-Jiménez, M., 2021. Supercontinuum source directly from noise-like pulse emission in a Tm-doped all-fiber laser with nonlinear polarization rotation. Results in Optics 2, 100040. https://doi.org/10.1016/j.rio.2020.100040.

Chen, Y., Chen, S., Liu, J., Gao, Y., Zhang, W., 2016. Sub-300 femtosecond soliton tunable fiber laser with all-anomalous dispersion passively mode locked by black phosphorus. Opt. Express 24 (12), 13316–13324. https://doi.org/10.1364/OE.24.013316.

Durán-Sánchez, M., Posada-Ramírez, B., Álvarez-Tamayo, R.I., Bello-Jiménez, M., García-Flores, Y.A., Armas-Rivera, I., Ibarra-Escamilla, B., 2020. Switchable dissipative soliton resonance and noise like pulses regimes in a mode-locked double-clad thulium doped fiber laser. Laser Phys. 31 (1), 015102 https://doi.org/10.1088/1555-6611/abd3f6.

Durán-Sánchez, M., Pottiez, O., Posada-Ramírez, B., Álvarez-Tamayo, R.I., Armas-Rivera, I., Bello-Jiménez, M., Ibarra-Escamilla, B., 2021. Multiple mode-locked regimes of an Er/Yb double-clad fiber laser based on NPR. J. Opt. 23 (4), 045501 https://doi.org/10.1088/2040-8986/abed5d.

Fried, N.M., Murray, K.E., 2005. High-power thulium fiber laser ablation of urinary tissues at 1.94 μm. J. Endourol. 19 (1), 25–31. https://doi.org/10.1089/end.2005.19.25.

Gaida, C., Gebhardt, M., Heuermann, T., Stutzki, F., Jauregui, C., Limpert, J., 2018. Ultrafast thulium fiber laser system emitting more than 1 kW of average power. Opt. Lett. 43 (23), 5853–5856. https://doi.org/10.1364/OL.43.005853.

Guo, Y.X., Li, X.H., Guo, P.L., Zheng, H.R., 2018. Supercontinuum generation in an Er-doped figure-eight passively mode-locked fiber laser. Opt. Express 26 (8), 9893–9900. https://doi.org/10.1364/OE.26.009893.

Hardy, L.A., Wilson, C.R., Irby, P.B., Fried, N.M., 2014. Rapid Thulium fiber laser lithotripsy at pulse rates up to 500 Hz using a stone basket. IEEE J. Sel. Top. Quantum Electron. 20 (5), 138–141. https://doi.org/10.1109/JSTQE.2014.2305715.

Huang, Y., Jivraj, J., Zhou, J., Ramjist, J., Wong, R., Gu, X., Yang, V.X., 2016. Pulsed and CW adjustable 1942 nm single-mode all-fiber Tm-doped fiber laser system for surgical laser soft tissue ablation applications. Opt. Express 24 (15), 16674–16686. https://doi.org/10.1364/OE.24.016674.

Ibarra Villalón, H.E., Pottiez, O., Bracamontes Rodriguez, Y.E., Lauterio-Cruz, J.P., Gomez Vieyra, A., 2018. Experimental study of non-stationary operation of a dual-wavelength passively mode-locked fibre ring laser. Laser Phys. 28 (6), 065103. https://doi.org/10.1088/1555-6611/aab65d.

Ibarra-Escamilla, B., Duran-Sanchez, M., Posada-Ramirez, B., Alvarez-Tamayo, R.I., Alaniz-Baylon, J., Bello-Jimenez, M., Prieto-Cortes, P., Kuzin, E.A., 2018. Passively Q-switched thulium-doped fiber laser using alcohol. IEEE Photonics Technol. Lett. 30 (20), 1768–1771. https://doi.org/10.1109/LPT.2018.2868923.

Kalaycıoğlu, H., Elahi, P., Akçaalan, Ö., Ilday, F.Ö., 2017. High-repetition-rate ultrafast fiber lasers for material processing. IEEE J. Sel. Top. Quantum Electron. 24 (3), 1–12. https://doi.org/10.1109/JSTQE.2017.2771745.

Kronenberg, P., Traxer, O., 2019. The laser of the future: reality and expectations about the new thulium fiber laser—a systematic review. Transl. Androl. Urol. 8 (S4), S398–S417.

Lekarev, V., Dymov, A., Vinarov, A., Sorokin, N., Minaev, V., Minaev, N., Tsypina, S., Yusupov, V., 2020. Mechanism of lithotripsy by superpulse thulium fiber laser and its clinical efficiency. Appl. Sci. 10 (21), 7480. https://doi.org/10.3390/app10217480.

Li, J., Yan, Z., Sun, Z., Luo, H., He, Y., Li, Z., Liu, Y., Zhang, L., 2014. Thulium-doped all-fiber mode-locked laser based on NPR and 45°-tilted fiber grating. Opt. Express 22 (25), 31020. https://doi.org/10.1364/OE.22.031020.

Liang, S., Xu, L., Fu, Q., Jung, Y., Shepherd, D.P., Richardson, D.J., Alam, S.U., 2018. 295-kW peak power picosecond pulses from a thulium-doped-fiber MOPA and the generation of watt-level> 2.5-octave supercontinuum extending up to 5 μm. Opt. Express 26 (6), 6490–6498. https://doi.org/10.1364/OE.26.006490.

Liao, R., Song, Y., Liu, W., Shi, H., Chai, L., Hu, M., 2018. Dual-comb spectroscopy with a single free-running thulium-doped fiber laser. Optics Express 26 (8), 11046–11054. https://doi.org/10.1364/OE.26.011046.

Lin, J.-H., Chen, C.-L., Chan, C.-W., Chang, W.-C., Chen, Y.-H., 2016. Investigation of noise-like pulses from a net normal Yb-doped fiber laser based on a nonlinear polarization rotation mechanism. Opt. Lett. 41 (22), 5310. https://doi.org/10.1364/OL.41.005310.

Liu, S., Yan, F.P., Zhang, L.N., Han, W.G., Bai, Z.Y., Zhou, H., 2015. Noise-like femtosecond pulse in passively mode-locked Tm-doped NALM-based oscillator with small net anomalous dispersion. J. Opt. 18 (1), 015508 https://doi.org/10.1088/2040-8978/18/1/015508.

Liu, S., Yan, F., Li, Y., Zhang, L., Bai, Z., Zhou, H., Hou, Y., 2016. Noise-like pulse generation from a thulium-doped fiber laser using nonlinear polarization rotation with different net anomalous dispersion. Photonics Res. 4 (6), 318–321. https://doi.org/10.1364/PRJ.4.000318.

Liu, S., Yan, F.-P., Feng, T., Zhang, L.-N., Bai, Z.-Y., Zhou, H., Hou, Y., Zhang, N., 2017. Single-polarization noise-like pulse generation from a hybrid mode-locked thulium-doped fiber laser. J. Opt. 19 (4), 045505. https://doi.org/10.1088/2040-8986/aa6267.

Ma, W., Wang, T., Su, Q., Wang, F., Zhang, J., Wang, C., Jiang, H., 2018. 1.9 μm square-wave passively Q-witched mode-locked fiber laser. Opt. Express 26 (10), 12514–12521. https://doi.org/10.1364/OE.26.012514.

Michalska, M., Swiderski, J., 2019. Noise-like pulse generation using polarization maintaining mode-locked thulium-doped fiber laser with nonlinear amplifying loop mirror. IEEE Photonics J. 11 (6), 1–10. https://doi.org/10.1109/JPHOT.2019.2943709.

Mingareev, I., Gehlich, N., Bonhoff, T., Abdulfattah, A., Sincore, A.M., Kadwani, P., Shah, L., Richardson, M., 2016. Principles and applications of trans-wafer processing using a 2-μm thulium fiber laser. Int. J. Adv. Manuf. Technol. 84 (9), 2567–2578. https://doi.org/10.1007/s00170-015-7870-z.

Olson, J., Ou, Y.H., Azarm, A., Kieu, K., 2018. Bi-directional mode-locked thulium fiber laser as a single-cavity dual-comb source. IEEE Photonics Technol. Lett. 30 (20), 1772–1775. https://doi.org/10.1109/LPT.2018.2868940.

Pottiez, O., Ibarra-Villalon, H.E., Bracamontes-Rodriguez, Y., Minguela-Gallardo, J.A., Garcia-Sanchez, E., Lauterio-Cruz, J.P., Hernandez-Garcia, J.C., Bello-Jimenez, M., Kuzin, E.A., 2017. Soliton formation from a noise-like pulse during extreme events in a fibre ring laser. Laser Phys. Lett. 14 (10), 105101. https://doi.org/10.1088/1612-202X/aa8298.

Ren, Z., Fu, Q., Xu, L., Price, J.H., Alam, S.U., Richardson, D.J., 2019. Compact, high repetition rate, 4.2 MW peak power, 1925 nm, thulium-doped fiber chirped-pulse amplification system with dissipative soliton seed laser. Opt. Express 27 (25), 36741–36749. https://doi.org/10.1364/OE.27.036741.

Rothman, L.S., Gordon, I.E., Babikov, Y., Barbe, A., Chris Benner, D., Bernath, P.F., Birk, M., Bizzocchi, L., Boudon, V., Brown, L.R., Campargue, A., Chance, K., Cohen, E.A., Coudert, L.H., Devi, V.M., Drouin, B.J., Fayt, A., Flaud, J.-M., Gamache, R.R., Harrison, J.J., Hartmann, J.-M., Hill, C., Hodges, J.T., Jacquemart, D., Jolly, A., Lamouroux, J., Le Roy, R.J., Li, G., Long, D.A., Lyulin, O. M., Mackie, C.J., Massie, S.T., Mikhailenko, S., Müller, H.S.P., Naumenko, O.V., Nikitin, A.V., Orphal, J., Perevalov, V., Perrin, A., Polovtseva, E.R., Richard, C., Smith, M.A.H., Starikova, E., Sung, K., Tashkun, S., Tennyson, J., Toon, G.C., Tyuterev, V.G., Wagner, G., 2013. The HITRAN2012 molecular spectroscopic database. J. Quant. Spectrosc. Radiat. Transfer 130, 4–50. https://doi.org/10.1016/j.jqsrt.2013.07.002.

Shtyrkova, K., Callahan, P.T., Li, N., Magden, E.S., Ruocco, A., Vermeulen, D., Ippen, E. P., 2019. Integrated CMOS-compatible Q-switched mode-locked lasers at 1900 nm with an on-chip artificial saturable absorber. Opt. Express 27 (3), 3542–3556. https://doi.org/10.1364/OE.27.003542.

Smirnov, S.V., Sugavanam, S., Gorbunov, O.A., Churkin, D.V., 2017. Generation of spatio-temporal extreme events in noise-like pulses NPE mode-locked fibre laser. Opt. Express 25 (19), 23122–23127. https://doi.org/10.1364/OE.25.023122.

Swiderski, J., Grzes, P., Michalska, M., 2021. Mid-infrared supercontinuum generation of 1.14 W in a fluoroindate fiber pumped by a fast gain-switched and mode-locked thulium-doped fiber laser system. Appl. Opt. 60 (9), 2647–2651. https://doi.org/10.1364/AO.422763.

Traxer*, O., Dymov, A., Rapoport, L., Tsarichenko, D., Enikeev, D., Sorokin, N., et al. (2019). V01-02 Comprehensive clinical study of super pulse tm fiber laser for treatment of stone disease. J. Urol., 201(Suppl. 4), e85-e86, 10.1097/01.JU.0000555074.09285.c7.

Traxer, O., Keller, E.X., 2019. Thulium fiber laser: the new player for kidney stone treatment? A comparison with Holmium: YAG laser. World J. Urol. 38 (8), 1883–1894. https://doi.org/10.1007/s00345-019-02654-5.

Ventimiglia, E., Doizi, S., Kovalenko, A., Andreeva, V., Traxer, O., 2020. Effect of temporal pulse shape on urinary stone phantom retropulsion rate and ablation efficiency using holmium: YAG and super-pulse thulium fibre lasers. BJU Int. 126 (1), 159–167. https://doi.org/10.1111/bju.v126.110.1111/bju.15079.

Voisiat, B., Gaponov, D., Gečys, P., Lavoute, L., Silva, M., Hideur, A., et al. (2015). Material processing with ultra-short pulse lasers working in 2μm wavelength range. In Laser Applications in Microelectronic and Optoelectronic Manufacturing (LAMOM) XX (Vol. 9350, p. 935014). International Society for Optics and Photonics, 10.1117/12.2078651.

Wang, J., Chen, H., Jiang, Z., Yin, J., Wang, J., Zhang, M., He, T., Li, J., Yan, P., Ruan, S., 2018. Mode-locked thulium-doped fiber laser with chemical vapor deposited molybdenum ditelluride. Opt. Lett. 43 (9), 1998. https://doi.org/10.1364/OL.43.001998.

Wang, M., Huang, S., Zeng, Y.J., Yang, J., Pei, J., Ruan, S., 2019. Passively Q-switched thulium-doped fiber laser based on oxygen vacancy MoO 3–x saturable absorber. Optical Materials Express 9 (11), 4429–4437. https://doi.org/10.1364/OME.9.004429.

Wang, X.F., Jin, Z.G., Liu, J.H., 2021. 2.04 μm harmonic noise-like pulses generation from a mode-locked fiber laser based on nonlinear polarization rotation. Optoelectron. Lett. 17 (1), 18–21. https://doi.org/10.1007/s11801-021-0028-3.

Wang, T., Ma, W., Jia, Q., Su, Q., Liu, P., Zhang, P., 2017. Passively mode-locked fiber lasers based on nonlinearity at 2-μm band. IEEE J. Sel. Top. Quantum Electron. 24 (3), 1–11. https://doi.org/10.1109/JSTQE.2017.2783047.

Wang, X.F., Mao, H.Y., Liu, Q.H., Liu, D.X., 2021. 2 μm noise-like mode-locked fiber laser based on non-linear optical loop mirror. Optoelectron. Lett. 17 (5), 294–297. https://doi.org/10.1007/s11801-021-0098-2.

Wang, Z., Wang, Z., Liu, Y.G., Zhao, W., Zhang, H., Wang, S., Yang, G., He, R., 2016. Q-switched-like soliton bunches and noise-like pulses generation in a partially mode-locked fiber laser. Opt. Express 24 (13), 14709. https://doi.org/10.1364/OE.24.014709.

Wang, Z., Wang, Z., Liu, Y.G., He, R., Wang, G., Yang, G., Han, S., 2018. The simultaneous generation of soliton bunches and Q-switched-like pulses in a partially mode-locked fiber laser with a graphene saturable absorber. Laser Phys. Lett. 15 (5), 055101. https://doi.org/10.1088/1612-202X/aaa142.

Zeng, J., Akosman, A.E., Sander, M.Y., 2019. Supercontinuum generation from a thulium ultrafast fiber laser in a high NA silica fiber. IEEE Photonics Technol. Lett. 31 (22), 1787–1790. https://doi.org/10.1109/LPT.6810.1109/LPT.2019.2946835.

Zhao, K., Wang, P., Ding, Y., Yao, S., Gui, L., Xiao, X., Yang, C., 2018. High-energy dissipative soliton resonance and rectangular noise-like pulse in a figure-9 Tm fiber

laser. Appl. Phys Express 12 (1), 012002. https://doi.org/10.7567/1882-0786/aaf0aa.